

# Optimal Trailing Edge Flap Positions of Helicopter Rotor for Various Thrust Coefficients to Solidity ( $C_t/\sigma$ ) Ratios

Saijal K. K., K. Prabhakaran Nair

**Abstract**—This study aims to determine change in optimal locations of dual trailing-edge flaps for various thrust coefficient to solidity ( $C_t/\sigma$ ) ratios of helicopter to achieve minimum hub vibration levels, with low penalty in terms of required trailing-edge flap control power. Polynomial response functions are used to approximate hub vibration and flap power objective functions. Single objective and multiobjective optimization is carried with the objective of minimizing hub vibration and flap power. The optimization result shows that the inboard flap location at low  $C_t/\sigma$  ratio move farther from the baseline value and at high  $C_t/\sigma$  ratio move towards the root of the blade for minimizing hub vibration.

**Keywords**—Helicopter rotor, Trailing-edge flap, Thrust coefficient to solidity ( $C_t/\sigma$ ) ratio, Optimization.

## I. INTRODUCTION

HELICOPTERS, with their hover, vertical takeoff/landing and forward flight capabilities, occupy a unique role in man-made flying vehicles. These unique flying characteristics, however, come at a price including complex aerodynamic problems, significant vibrations, high levels of noise, and relatively large power requirements compared to a fixed-wing aircraft of the same weight. High noise levels greatly restrict the use of helicopters over densely-populated and urban areas. High vibration levels directly lead to passenger discomfort and high maintenance cost. These high vibration levels compared to other flying vehicles is mainly because of the highly unsteady aerodynamic environment around the rotor and the flexibility of the long slender rotor blades [1]. The high vibration creates a hostile environment for the electronics and other equipment on board, making it difficult to read the instruments leading to inaccurate weapon delivery. The impact of these high vibration levels on passenger and crew comfort is also critical. Therefore, considerable efforts are made to reduce vibration levels in helicopters. The primary sources of vibration in the helicopter are main rotor system, the aerodynamic interaction between the rotor and the fuselage, the tail rotor, the engine, and the transmission. The main rotor is the most significant source of vibration because of the highly unsteady aerodynamic environment acting on highly flexible rotating blades.

Saijal K. K. is Research Scholar, Kozhikode, Kerala, National Institute of Technology Calicut, India (e-mail: saijalkk@gmail.com).

K. Prabhakaran Nair is with the Department of Mechanical Engineering, National Institute of Technology Calicut, Kerala, India (e-mail: kpn@nitc.ac.in).

Passive vibration control devices such as dynamic vibration absorber and isolation mounting in helicopters are not found to be effective and efficient for the desired comfort level in rotorcraft flight. These devices are tuned for a particular cruise condition and cannot be changed once the rotor is in operation.

Another drawback is the large weight penalty associated with these devices. The isolation system may cause large structural deflection during maneuver or transient flight condition. The dynamic pendulum absorbers mounted on the rotor blade may also add to the drag penalty of the helicopter [2]. Therefore, researchers have turned towards the active vibration control approach in the past decade.

Higher Harmonic Control (HHC) is one of the rotor-based active control approaches in which vibration is suppressed at the source through excitation of the blade pitch at higher harmonics of the rotational speed. The HHC concept has been investigated through numerical simulations [3] and wind tunnel tests [4]. But the actuation system in this case is limited to  $N_b$ /rev excitation frequencies for an  $N_b$  bladed rotor. This can be resolved by the use of Individual Blade Control (IBC) [5], [6] in which each blade is individually controlled in the rotating frame over a wide range of desired frequencies. HHC and IBC have the potential for substantial vibration reduction, but both approaches have limitations in their practical implementations. Both of these methods have considerable weight penalties and high cost. Moreover, large actuation power is needed to pitch the entire blade and complex actuation system.

With the advancements in smart materials technology, especially piezoelectric materials, actively controlled trailing-edge flaps have been proposed as a low power localized actuator system to achieve individual blade control. In this method, one or more on-blade trailing-edge flaps, each of them spanning about 4-6 percent of the blade are actuated. This approach substantially reduces the control power for actuation when compared to HHC and IBC. Actively controlled trailing-edge flaps represent one of the most promising methods for vibration reduction in helicopters because of low power consumption, light weight, compact size, airworthiness and high adaptation. The potential of trailing-edge flap concept to reduce the vibratory hub loads, alleviate noise and enhance rotor performance has been demonstrated by several numerical [7], [8] and experimental [9], [10] investigations. Piezostack-based actuators are best suited for the actuation of trailing-edge flaps in full-scale

rotor blades. Studies show that the multiple flaps are capable of achieving higher vibration reduction compared to single flap configuration within available actuator authority [11], [12]. Response surface approximation has found wide applications in complex design optimization problems [1]. Comparative studies show that RSM is ideal for [13], [14] small scale, non linear problems [15], [16] used RSM for optimum design of helicopter rotor for low vibration taking the flap bending, lag bending and torsion stiffness as design variables. The use of RSM in helicopter rotor optimization is again demonstrated by Viswamurthy and Ganguli [17] in their work on the optimum placement of dual trailing-edge flaps for low vibration with minimum flap control power and Saijal et al. [18] in their work on the Optimization of Helicopter Rotor Using Polynomial and Neural Network Meta- models. These studies show the potential of RSM to decouple complicated helicopter aeroelastic analysis and optimization problem.

This work investigates the change in optimal locations of dual trailing-edge flaps for minimum vibration and flap control power for various thrust coefficients to solidity ( $C_t/\sigma$ ) ratios of helicopter. Polynomial response functions are used to approximate the hub vibration and flap control power objective functions.

## II. OPTIMIZATION PROBLEM

The present study aims to find the optimal locations of the trailing-edge flaps to achieve maximum reduction in hub vibration with minimum penalty in terms of power consumed by the active flap system, for various thrust coefficients to solidity ( $C_t/\sigma$ ) ratios of helicopter. The hub vibration and flap power objective functions are normalized with respect to their corresponding values at the baseline configuration. These normalized values are denoted by  $F_v$  and  $F_p$ , respectively. The design variables considered for this study are the inboard flap position,  $x_1$  and outboard flap position,  $x_2$ . Constraints are imposed on the upper and lower bounds of the design variables (move limits). The numerical values for initial configuration and move limits for variables  $x_1$  and  $x_2$  are given in Table I. The inboard and outboard flaps are constrained to be placed between 59 to 71 and 77 to 89 percent blade.

TABLE I  
INITIAL CONFIGURATION AND MOVABLE LIMITS

Design variable	Lower limit	Baseline value	Upper limit
$x_1$	.59R	.65R	.71R
$x_2$	.77R	.85R	.89R

Minimize  $\{F_v, F_p\}$

$$\begin{aligned} \text{Subject to : } & x_1 - \text{lower} \leq x_1 \leq \\ & x_1 - \text{upper} \\ & x_2 - \text{lower} \leq x_2 \leq \\ & x_2 - \text{upper} \end{aligned}$$

This is a multi-objective optimization problem with constraints. The nature of the tradeoff between the two objectives depends on the shape of Pareto curve/surface. A solution is said to be Pareto optimal if it is impossible to

minimize any one objective without allowing an increase in one or more of the other objectives.

## III. NUMERICAL RESULTS

Numerical results are obtained for a four bladed, soft inplane, uniform hingeless rotor with twin trailing-edge flaps. The trailing-edge flaps considered in this study are plain flaps where the flap is integrated into the airfoil cross-section. This study is conducted at thrust coefficient to solidity ratios,  $C_t/\sigma = 0.04, 0.07$  and  $0.10$  using an aeroelastic analysis based on finite elements in space and time. A coupled trim procedure is used for solving the rotor blade response and trim equations simultaneously. Using the helicopter aeroelastic analysis, the hub vibration objective function  $F_v$  and flap control power objective function  $F_p$  are evaluated at the data points corresponding to Central Composite Design (CCD). The response surfaces are obtained by minimizing the error square for both objective functions at thrust coefficient to solidity ratios,  $C_t/\sigma = 0.04, 0.07$  and  $0.10$ .

Firstly, a single objective optimization is conducted using the response surface functions. An exhaustive search conducted in the design space using the  $F_v$  response surface with the objective of minimizing the hub vibration. Similarly, an exhaustive search with the objective of minimizing flap power alone is also conducted. The results are given in Table II.

TABLE II  
OPTIMAL TRAILING-EDGE FLAP LOCATIONS FOR VARIOUS THRUST COEFFICIENT TO SOLIDITY ( $C_t/\sigma$ ) RATIOS

Thrust coefficient Ratio	Optimum flap positions for minimizing $F_v$ alone		Optimum flap positions for minimizing $F_p$ alone	
	$x_1$	$x_2$	$x_1$	$x_2$
.04	.68R	.89R	.71R	.77R
.07	.65R	.89R	.71R	.77R
1.0	.64R	.89R	.71R	.77R

The optimization results shows that the inboard flap location changes from 0.68R to 0.64R as the thrust coefficient to solidity ( $C_t/\sigma$ ) ratio varies from 0.04 to 0.10. It is seen that the inboard flap location moves towards the root of the blade with increase in  $C_t/\sigma$ . Optimum outboard flap position is at the upper limit for single objective optimization minimizing hub vibration,  $F_v$  alone for all  $C_t/\sigma$  ratios. The variation of optimum positions of inboard and outboard flap for minimizing hub vibration alone is shown in Fig. 1. Single objective optimization minimizing flap power alone gives exactly same optimum flap positions for all thrust coefficient to solidity ( $C_t/\sigma$ ) ratios ( $x_1=0.71R, x_2=0.77R$ ). This shows that the optimal flap locations for single objective optimization are different for the two objective functions.

Figs. 2, 3 show the variation in hub vibration,  $F_v$  and flap power,  $F_p$ , with respect to inboard flap position,  $x_1$  and outboard flap position,  $x_2$  for thrust coefficient to solidity ratios,  $C_t/\sigma = 0.04$  and  $C_t/\sigma = 0.10$ . From these figures, it can be seen that the variation in hub vibration and flap

power with respect to flap positions are almost similar for these thrust coefficient to solidity ratios. This is the reason for not having major changes in optimum for flap locations in single objective optimization at various thrust coefficients to solidity ratios.

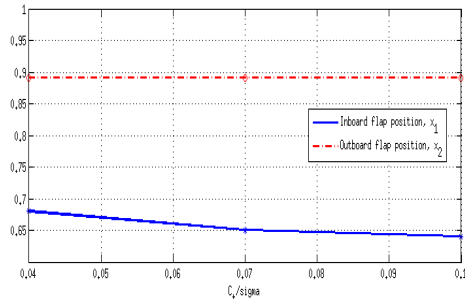


Fig. 1 Optimum flap positions to minimize hub vibration alone for various thrust coefficients to solidity ( $C_t/\sigma$ ) ratios

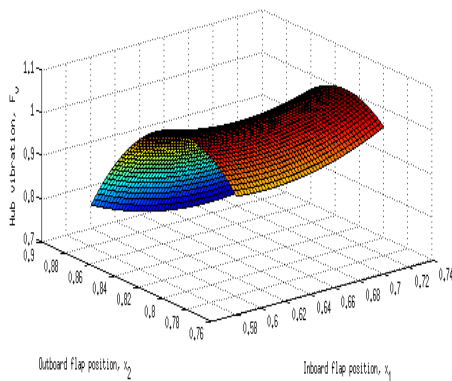


Fig. 2 Variation in hub vibration,  $F_v$  with respect to inboard flap position,  $x_1$  and outboard flap position,  $x_2$  for thrust coefficient to solidity ratios  $C_t/\sigma = 0.04$

The optimization results shows that the inboard flap location changes from 0.68R to 0.64R as the thrust coefficient to solidity ( $C_t/\sigma$ ) ratio varies from 0.04 to 0.10. It is seen that the inboard flap location moves towards the root of the blade with increase in  $C_t/\sigma$ . Optimum outboard flap position is at the upper limit for single objective optimization minimizing hub vibration,  $F_v$  alone for all  $C_t/\sigma$  ratios. The variation of optimum positions of inboard and outboard flap for minimizing hub vibration alone is shown in Fig. 1. Single objective optimization minimizing flap power alone gives exactly same optimum flap positions for all thrust coefficient to solidity ( $C_t/\sigma$ ) ratios ( $x_1=0.71R$ ,  $x_2=0.77R$ ). This shows that the optimal flap locations for single objective optimization are different for the two objective functions.

Figs. 2, 3 show the variation in hub vibration,  $F_v$  and flap power,  $F_p$ , with respect to inboard flap position,  $x_1$  and outboard flap position,  $x_2$  for thrust coefficient to solidity ratios,  $C_t/\sigma = 0.04$  and  $C_t/\sigma = 0.10$ . From these figures,

it can be seen that the variation in hub vibration and flap power with respect to flap positions are almost similar for these thrust coefficient to solidity ratios. This is the reason for not having major changes in optimum for flap locations in single objective optimization at various thrust coefficients to solidity ratios

Because of the conflicting nature of the requirement, 'compromise design' which will minimize both vibration levels and trailing-edge flap power at various thrust coefficients to solidity ratios are also explored. Fig. 4 shows the hub vibration levels and trailing-edge flap power resulting from various design choices within the move limits for thrust coefficient to solidity ratio,  $C_t/\sigma = 0.04$ . It is obtained by moving from design space ( $x_1, x_2$ ) to criterion space ( $F_v, F_p$ ) using response surface metamodel. The design point  $F_v = F_p = 1$  corresponds to the initial design point (baseline value). It is seen that the Pareto surface is divided into two distinct parts with no feasible design point lying in the 'compromise region'.

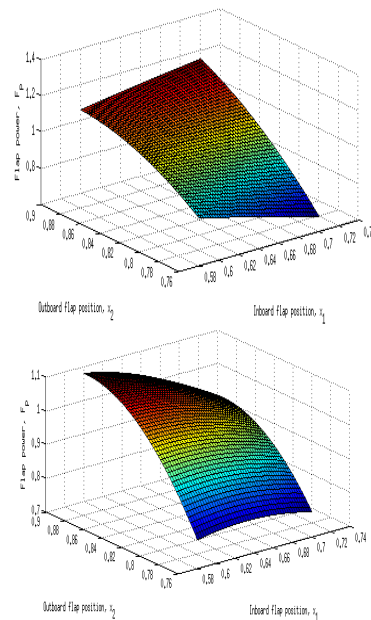


Fig. 3 Variation in Flap power,  $F_p$  with respect to inboard flap position,  $x_1$  and outboard flap position,  $x_2$  for thrust coefficient to solidity ratios  $C_t/\sigma = 0.04$  and  $C_t/\sigma = 0.10$

Design point A corresponds to  $(x_1, x_2)=(0.68R, 0.89R)$ , which is same as the optimum obtained in single objective optimization with the objective of minimizing  $F_v$  alone. Design point B corresponds to  $(x_1, x_2)=(0.71R, 0.77R)$ , which is same as the optimum obtained in single objective optimization with the objective of minimizing  $F_p$  alone. Similarly, Fig. 4 shows the hub vibration levels and trailing-edge flap power resulting from various design choices within the move limits for thrust coefficient to solidity ratio,  $C_t/\sigma = 0.10$ . Design point C corresponds to  $(x_1, x_2)=(0.64R, 0.89R)$ , which is very near to the optimum obtained in single objective

optimization with the objective of minimizing  $F_v$  alone. Design point D corresponds to  $(x_1, x_2)=(0.71R, 0.77R)$ , which is exactly same as the optimum obtained in single objective optimization with the objective of minimizing,  $F_p$  alone.

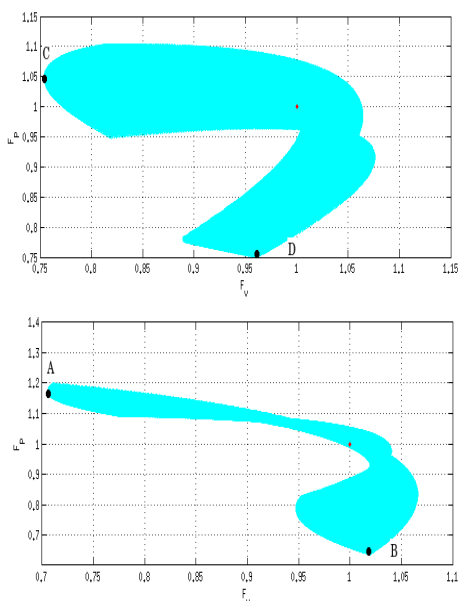


Fig. 4  $F_v$  versus  $F_p$  for various design points within the move limits

#### IV. CONCLUSION

Optimization results for the placement of dual trailing edge flaps are obtained for low hub vibration with minimum flap control power for advance ratios corresponding to various thrust coefficients to solidity ( $C_t/\sigma$ ) ratios of helicopter. Polynomial response functions are used to approximate the objectives. The following conclusions can be made from this study.

1. Single objective optimization with the objective of minimizing hub vibration alone shows the inboard flap location moves towards the root of the blade with increase in thrust coefficient to solidity ( $C_t/\sigma$ ) ratios.
2. Single objective optimization with the objective of minimizing flap power alone gives exactly same optimum flap locations for all advance ratios.
3. Multiobjective optimization with the objective of minimizing hub vibration and flap power for thrust coefficient to solidity ratios of  $C_t/\sigma = 0.04$  and  $C_t/\sigma = 0.10$  gives similar Pareto surface. The Pareto surfaces in the both cases are disjoint, not giving a 'compromise design' point.
4. From the results of single objective optimization and multiobjective optimization, it can be seen that there is not much change in the optimum flap locations with advance ratios corresponding to various cruise speeds of helicopter. This result is helpful in fixing the position of trailing-edge flaps in helicopter rotor blade.

#### REFERENCES

- [1] P.P. Friedmann, The Renaissance of Aeroelasticity and its Future, Vol 37, pp.105-121, Journal of Aircraft, 1999.
- [2] R. Loewy, Helicopter Vibrations: A Technological Perspective, 43(4), pp.4-30, Journal of American Helicopter Society, 1984.
- [3] K. Nguyen and I. Chopra, Application of Higher Harmonic Control to Rotors Operating at High Speed and Maneuvering Flight, 35, pp.78-89, Journal of American Helicopter Society, 1990.
- [4] C.E. Hammond, Wind Tunnel Results Showing Rotor Vibratory Loads Reduction Using Higher Harmonic Blade Pitch, 28, pp.9-15, Journal of American Helicopter Society, 1983.
- [5] K.F. Guinn, Individual Blade Control Independent of a Swashplate, 25-31, Journal of American Helicopter Society, 1982.
- [6] N.D. Ham, A Simple System for Helicopter Individual Blade Control Using Modal Decomposition, Vol 4, pp.23-28, Vertica, 1980.
- [7] J. Milgram, I. Chopra and F.K. Straub, Rotors with Trailing Edge Flap: Analysis and Comparison with Experimental Data, 43(4), pp.319-332, Journal of American Helicopter Society, 1998.
- [8] P.P. Friedmann, M. De Terlizzi and T.F. Myrtle, New Developments in Vibration Reduction with Actively Controlled Trailing Edge Flaps, 33(10-11), pp.1055-1083, Math. Comput. Model., 2001.
- [9] M.V. Fulton and R.A. Ormiston, Hover Testing of a Small Scale Rotor with On-blade Elevons, 46(2), pp.96-106, Journal of American Helicopter Society, 2001.
- [10] N. Koratkar and I. Chopra, Closed-loop wind tunnel testing of a smart rotor model with trailing edge flaps, 47(4), pp.263-272, Journal of American Helicopter Society, 2002.
- [11] S.R. Viswamurthy and R. Ganguli, An Optimization Approach to Vibration Reduction in Helicopter Rotors with Multiple Active Trailing Edge Flaps, 8(3), pp.185-194, Aerosp. Sci. Technol., 2004.
- [12] J.S. Kim, E.C. Smith and K.W. Wang, Helicopter Vibration Suppression via Multiple Trailing Edge Flaps Controlled by Resonance Actuation System, pp.7-10, Paper presented at the American Helicopter Society 60th Annual Forum, Baltimore, Maryland, USA, 2004.
- [13] H. Agarwal and J.E. Renaud, Reliability Based Design Optimization Using Response Surfaces in Application to Multidisciplinary Systems, 36(3), pp.291-311, Engineering Optimization, 2004.
- [14] S. Venkataraman, Reliability Optimization Using Probabilistic Sufficiency Factor and Correction Response Surface, 38(6), pp.671-685, Engineering Optimization, 2006.
- [15] R. Jin, W. Chen and T.W. Simpson, Comparative Studies of Meta-modelling Techniques under Multiple Modelling Criteria, 23(1), pp.1-13, Structural Multidisciplinary Optimization, 2001.
- [16] R. Ganguli, Optimum Design of a Helicopter Rotor for Low Vibration Using Aeroelastic Analysis and Response Surface Methods, 258(2), pp.327-344, Journal of Sound and Vibration, 2002.
- [17] S.R. Viswamurthy and R. Ganguli, Optimal Placement of Trailing-edge flaps for Helicopter Vibration Reduction Using Response Surface Methods, Vol.39, No.2, pp.185-202, Engineering Optimization, 2007.
- [18] K.K. Sajjal, R. Ganguli and S.R. Viswamurthy, Optimization of Helicopter Rotor Using Polynomial and Neural Network Metamodels, Vol.48, No.2, pp.553-566, Journal of Aircraft, 2011.